# UC San Diego
## UC San Diego Electronic Theses and Dissertations

**Title**
Self-Assembling Lipopeptide Nanocarriers for Targeted Cellular Uptake

**Permalink**
https://escholarship.org/uc/item/0wt744vt

**Author**
Cho, Christy Jihyun

**Publication Date**
2019

Peer reviewed|Thesis/dissertation

UNIVERSITY OF CALIFORNIA SAN DIEGO


Self-Assembling Lipopeptide Nanocarriers for Targeted Cellular Uptake


A Thesis submitted in partial satisfaction of the requirements
for the degree Master of Science


in


Chemistry


by


Christy Jihyun Cho


Committee in charge:

      Professor Neal K. Devaraj, Chair
      Professor Elizabeth Komives
      Professor Francesco Paesani


2019

The Thesis of Christy Jihyun Cho is approved, and it is acceptable in quality and form

for publication on microfilm and electronically:

_____

_____

_____

Chair

University of California San Diego

2019

DEDICATION

*This thesis is dedicated to my family,*

*without whom nothing would have been possible.*

*My parents,*

*Mr. & Mrs. Kwan Hyun "John" and Jeong Hee "Rufina" Cho,*

*to whom I owe everything.*

*Without your sacrifices, none of this would have been made possible.*

*Thank you for your endless prayers, unconditional love, and support.*

*My little brother Min Geun Daniel Cho,*

*I am deeply grateful for being a kind-hearted, intelligent, and loving brother. You have always*

*been the older brother to me, although you will forever be my baby brother.*

*I am honored to be your sister. I love you.*

*&*

*My beloved Grandparents,*

*Young Geum Kam*          *Won Rae Cho*

*(1930, May 07 ~ 2015, Feburary 20)*     *(1929, August 20 ~ 2016, January 23)*

*Words cannot express how much I love you and miss you. I will never let go of the values you*

*have instilled in me. You will be dearly missed and forever loved. Most importantly,*

*you will live on in my heart and in my work.*

TABLE OF CONTENTS

# LIST OF ABBREVIATIONS

| | |
|---|---|
| Alloc | allyloxycarbonyl |
| Boc | *tert*-butoxycarbonyl |
| C | cysteine (Cys) |
| $C_{18:1}$ | oleoyl |
| CLSM | confocal laser scanning microscopy |
| CTC | 2-chlorotrityl chloride |
| D | aspartic Acid (Asp) |
| DIPEA | *N,N*-diisopropylethylamine |
| DOX | doxorubicin |
| EDT | ethanedithiol |
| ELSD | evaporative light-scattering detection |
| f | *D*-phenylalanine (*D*-Phe) |
| FBS | fetal bovine serum |
| Fmoc | 9-fluorenylmethoxycarbonyl |
| G | glycine (Gly) |
| H | histidine (His) |
| HATU | 1-[bis(dimethylamino)methylene]-1H-1,2,3-triazolo[4,5-b]pyridinium 3-oxide hexafluorophosphate |
| HBTU | 2,2,4,6,7-tetramethyluronium hexafluorophosphate |
| HFIP | 1,1,1,3,3,3-hexafluoro-2-propanol |
| HOBt | 1-hydroxybenzotriazole |

| | |
|---|---|
| HPLC | high-performance liquid chromatography |
| K | lysine (Lys) |
| LC | liquid chromatography |
| LP | lipopeptide |
| MESNA | sodium 2-mercaptoethanesulfonate |
| MS | mass spectrometry |
| NCL | native chemical ligation |
| PBS | phosphate-buffered saline |
| PEG | polyethylene glycol |
| SPPS | solid-phase peptide synthesis |
| sfGFP | superfolder green fluorescence protein |
| TCEP.HCl | tris(2-carboxyethyl)phosphine hydrochloride |
| TEM | transmission electron microscopy |
| *t*Bu | *tert*-butyl |
| TFA | trifluoroacetic acid |
| Tris | tris(hydroxymethyl)aminomethane |
| Trt | trityl |

# LIST OF FIGURES

# LIST OF TABLES

# ACKNOWLEDGEMENTS

ABSTRACT OF THE THESIS


Self-Assembling Lipopeptide Nanocarriers for Targeted Cellular Uptake

by


Christy Jihyun Cho

Master of Science in Chemistry

University of California San Diego, 2019

Professor Neal K. Devaraj, Chair

Self-assembling lipopeptide nanocarriers have emerged as one of the most powerful delivery vehicles, providing unique opportunities to transport therapeutic drugs. In efforts to improve target specificity, such carriers are functionalized with integrin-binding motifs (such as RGD peptide sequences), enhancing cellular uptake via ligand-receptor interactions. However, common approaches for the preparation of the desired structures require complex synthetic routes

to covalently conjugate the peptide ligands to the lipid fragments. It would be thus valuable to develop a straightforward methodology to construct biocompatible vehicles that can efficiently deliver functional cargos to live cells. Herein, we describe a new class of nanocarrier systems constituted by self-assembling lipopeptides conjugated with specific integrin-binding motifs. The approach takes advantage of chemoselective and non-enzymatic methods to synthesize functional lipopeptides, which spontaneously self-assemble into micron-sized vesicles. The straightforward construction of our model systems, jointly with their robustness, biocompatibility and simplicity, highlights their relevant use as carriers for the enhanced cellular uptake of fluorescently labeled biomacromolecules (Texas Red-Dextran) and therapeutic agents (doxorubicin) via receptor-mediated endocytosis pathway.

# 1. INTRODUCTION

In the last decade, the field of nanomedicine has undergone explosive growth, with applications stretching from targeted drug delivery systems to the construction of biological nanodevices.[1] Specifically, this field has been developed to overcome current limitations in disease treatments such as low specificity, high toxicity, and biocompatibility.[2] For instance, nanomedicine diagnostics can provide early detection of cancers for a more efficient treatment.[3] Current platforms of nanomedicine for drug delivery systems utilize nanocontainers to protect relevant biomolecules or therapeutic agents from rapid degradation and increase their efficiency. Additionally, small-molecule cargos generally have short circulation half-lives, and therefore nanocarriers with improved bioavailability and efficacy are needed.[4]

A variety of complex nanocarriers have been used as drug delivery systems, including polymeric nanostructures, metallic nanoparticles, and lipid-based assemblies.[1] With the help of such nanocarriers, small-molecule drugs can overcome problems of stability, solubility, and nonspecific toxicity, by being delivered the intended target directly. Polymeric nanoparticles are colloidal structures composed of biocompatible polymers.[5] Such materials are designed to entrap molecules of interest and efficiently deliver them to certain targets of choice. Remarkably, the established cavities can improve the bioavailability of hydrophobic drugs and therapeutic effects. Polymer-based nanoparticles, however, do not degrade easily over time, which severely limits their applicability as drug delivery systems in mammalian tissues. Recently, inorganic nanoparticles have been used as effective nanocarriers due to their unique properties as fluorescent markers.[6] For instance, quantum dots, a new class of semiconductor nanocrystals composed of inorganic elemental cores, are used both as powerful fluorescent labels.[7] The main drawbacks of

using inorganic nanoparticles, is toxicity, making it necessary to coat the outer shell with biocompatible materials.

Lipid-based assemblies, either micelles or liposomes, have been widely used as simple nanocarrier model systems.[8,9] Lipid micelles are formed by amphiphiles that associate into structures containing a hydrophobic core and a hydrophilic shell.[8] However, one of their common drawbacks is that they can only encapsulate hydrophobic molecules, limiting their applicability. On the other hand, liposomes are comprised of amphiphiles that self-assemble to form lipid bilayers with an aqueous core.[9] They offer improved solubility of the therapeutic agents, biodegradability, and efficacy by reducing nonspecific toxicity of the encapsulated material. Liposomes are also relatively easy to synthesize when compared to synthetic polymer-based nanoparticles or metallic nanostructures.

One of the key features for the design of an ideal delivery system is the incorporation of functional moieties that allow an optimal cellular uptake. Nanocarriers may be modified to employ passive and active targeting pathways to reach tumor tissue. Through enhanced permeability and retention effects (EPR), nanocarriers are allowed to passively buildup in tissues, such as liver and spleen.[4] This pathway, however, does not efficiently eliminate such nanostructures from the sites of accumulation. Active targeting uses attachments of ligands to the surface of nanocarriers to obtain high specificity to receptors.[10] This eliminates nonspecific uptake of nanocarriers other than the tissue of choice. For instance, incorporation of cell-binding motifs enhances active targeting pathway via ligand-receptor interactions. Among these motifs, the trimer sequence RGD functions as an effective targeting agent recognized and internalized by well-known tumor-associated receptors, $\alpha_v\beta_3$ and $\alpha_v\beta_5$ integrins.[11] The $\alpha_v\beta_3$ integrins are of particular interest since they are

overexpressed in vessels and a quarter of mammalian (human) cancer cells such as glioblastomas, melanoma, prostate, breast, and ovarian cancer.[12]

Modification of liposomes with integrin-binding motifs promotes specific cellular uptake via receptor-mediated endocytosis, which is not possible with single peptide constructs or non-targeted nanocarriers. Lipidation of peptides offers a significant class of self-assembling molecules capable of forming peptide-functionalized nanostructures. The self-assembled nanostructures consist of peptide moieties on the surface, which makes these targeted liposomes. Thus, the delivery of drugs is enhanced by selectively binding to $\alpha_v\beta_3$ overexpressed cancer cells. For instance, RGD-based nanocarriers conjugated with anticancer drugs such as doxorubicin (DOX) have been shown to have improved specificity for therapeutic activity *in vitro* and *in vivo* relative to corresponding free drugs.[12] DOX is a powerful, nonspecific therapeutic agent that leads to cell death in cancerous as well as non-cancerous cells or tissues.[13] Previous studies have demonstrated that DOX can either be encapsulated[13] or conjugated onto the surface of polymers/carriers via covalent linkage.[14] This linkage offers stable conjugates, but the formation process requires complex synthetic routes. Additionally, it must be carefully chosen since the covalent bonds need to be cleaved and the therapeutic agents released under physiological conditions. One of the common methods, PEGylation of RGD, has been extensively used to physically encapsulate DOX and improve biocompatibility of the nanocarriers.[15] However, effective delivery of the therapeutic agent still remains challenging and limited in scope. Therefore, it would be valuable to develop a straightforward methodology to construct biocompatible nanocarriers that can efficiently deliver functional cargos in live cells. Herein, we describe a new class of nanocarrier systems constituted by self-assembling lipopeptides (LPs) conjugated with the trimeric sequence RGD (Figure 1). Our approach takes advantage of the native chemical ligation (NCL)[16,17] to synthesize functional

lipopeptide conjugates, which spontaneously self-assemble into micron-sized vesicles. Remarkably, the RGD sequence of the resulting lipopeptide vesicular structures can target $\alpha_v\beta_3$ integrin-overexpressing cancer cells without the need of PEGylation to encapsulate and deliver the entrapped biomolecules. The straightforward construction of our model systems, jointly with their robustness, biocompatibility and simplicity, highlights their relevant use as effective delivery vehicles for the enhanced cellular uptake of relevant biomacromolecules (dextrans) and therapeutic agents (DOX) via receptor-mediated endocytic pathway.
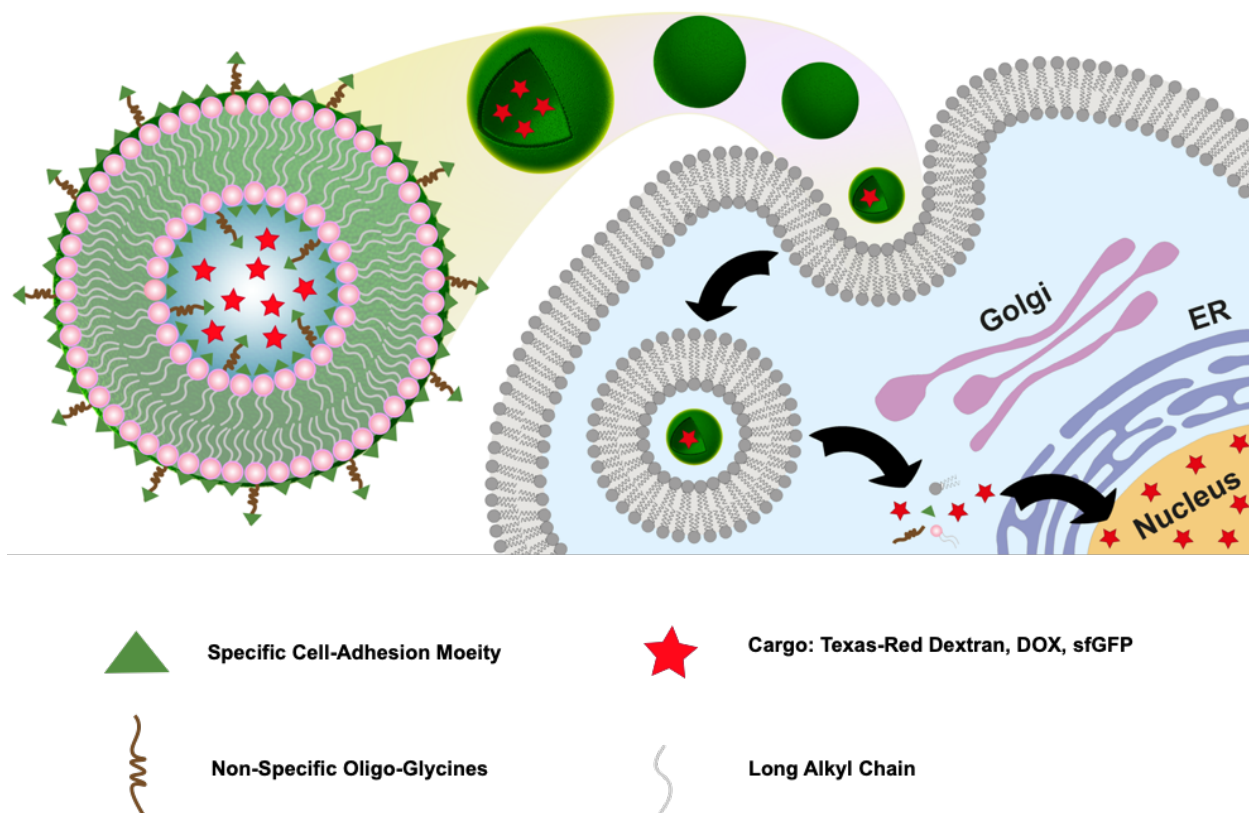


**Figure 1.** Schematic representation of the receptor-mediated endocytosis pathway for a new class of self-assembling lipopeptide nanocarriers. Upon recognition of the specific integrins, nanocarriers are internalized and can then traffic into endosomes. Degradation at lower pH allows the release of entrapped cargo into the cytoplasm, ultimately being delivered to the nucleus.

## 2. RESULTS AND DISCUSSION

### 2.1. Construction of Self-Assembling Lipopeptides via Native Chemical Ligation (NCL)
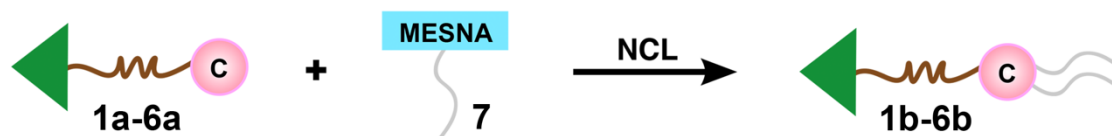
NCL is a well-established non-enzymatic and chemoselective methodology for the construction of relevant biomolecules, such as polypeptides, proteins, and nucleic acids.[16,17] We have recently expanded the application of the NCL to the formation of artificial membranes.[18] This catalyst-free strategy was employed to generate phospholipids *in situ* from water-soluble long-chain thioesters. The lipids were capable of spontaneous self-assembly into vesicles that can grow to several microns in diameter. Using a similar NCL methodology, we have designed a novel strategy to prepare functional lipopeptide nanocarriers (Figure 2, Table 1). Our approach was based on the N- and S-lipidation of various N-terminal cysteine-based peptides (**1a-6a**) with long-chain thioesters in aqueous solution. All peptides were synthesized by using standard solid-phase peptide synthesis (SPPS) protocols.[19] The peptides (2.5 mM) were reacted overnight with oleoyl sodium 2-mercaptoethanesulfonate (MESNA)[18] [**7**] (5 mM) in tris(hydroxymethyl)aminomethane (Tris) buffer solution, pH 8.0 containing tris(2-carboxyethyl)phosphine hydrochloride (TCEP.HCl) (10 mM). Initial transthioesterification between the free thiol group of the N-terminal cysteine residue and **7** results in a thioester intermediate that undergoes spontaneous rearrangement via nucleophilic attack by the amino group to form the native amide bond. The excess of **7** allows for a subsequent "reloading" step that generates a second oleoyl tail on the peptide as a result of the formation of a new thioester linkage. Remarkably, with the limited observable thioester-linked intermediate ligation product, it is plausible that the rate-limiting step is the transthioesterification with the thiol moiety of the side chain of the N-terminal cysteine. The formation of the double-chain peptide

amphiphiles (**1b-6b**) was analyzed over time using combined liquid chromatography (LC), mass spectrometry (MS), and evaporative light-scattering detection (ELSD) measurements.
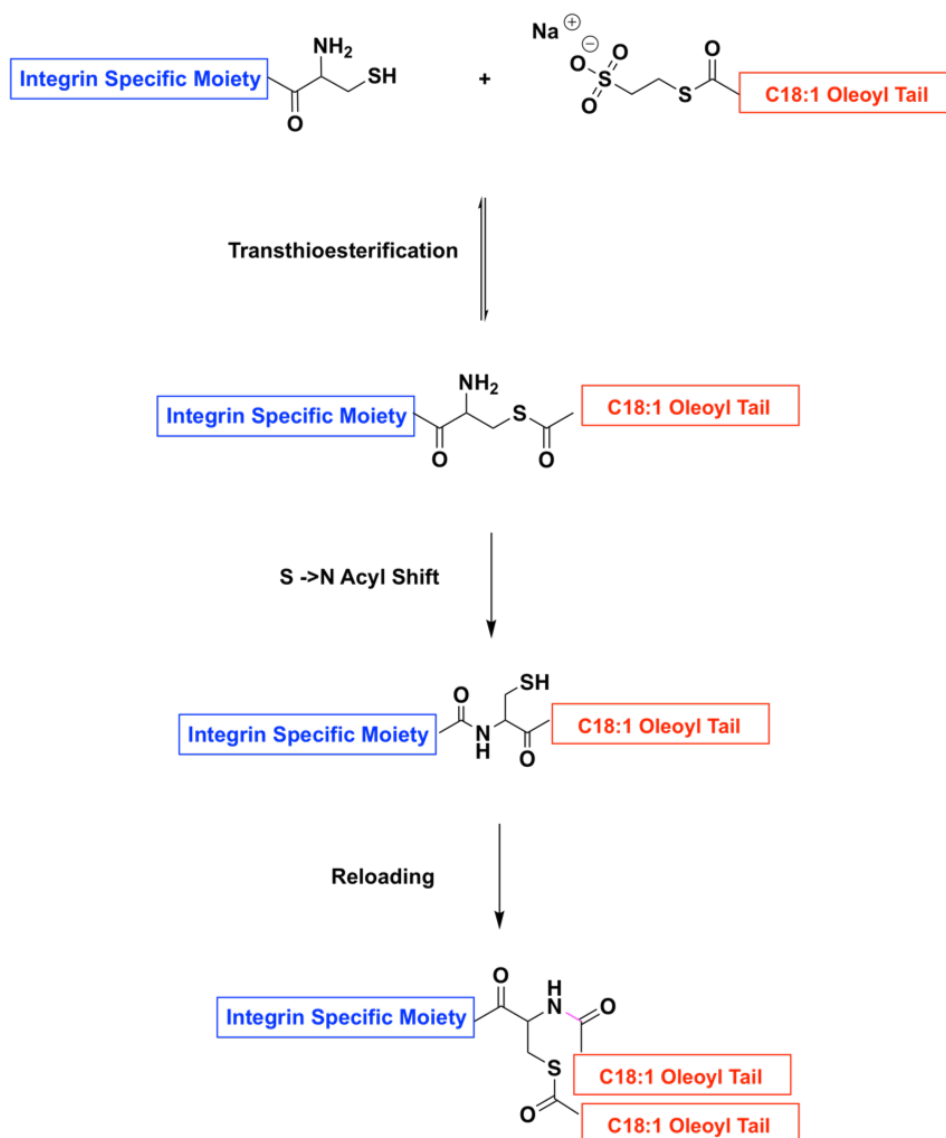


**Figure 2.** NCL mechanism showing the formation of a new class of dioleoyl-peptides. The mechanism NCL involves a two-step process consisting of a thiol-exchange step between a C-terminal MESNA thioester and the sulfhydryl moiety of an N-terminal cysteine peptide, which prompts an intramolecular nucleophilic attack by the α-amino group of the cysteine to form the final amide bond.

**Table 1.** List of peptides (**1a-6a**) and lipopeptides (**1b-6b**) used in this study. *Top,* schematic representation of NCL reaction between N-terminal cysteine-containing peptides and MESNA oleoyl thioester (**7**), affording the corresponding dioleoyl lipopeptides.



| Compound | ▲ | 〰 | 〜 |
|----------|-----------|--------|--------------|
| 1a | RGD | - | - |
| 1b | RGD | - | $C_{18:1}$ |
| 2a | GHK | - | |
| 2b | GHK | - | $C_{18:1}$ |
| 3a | RGD | GGG | - |
| 3b | RGD | GGG | $C_{18:1}$ |
| 4a | GHK | GGG | - |
| 4b | GHK | GGG | $C_{18:1}$ |
| 5a | RGD | GGGGG | - |
| 5b | RGD | GGGGG | $C_{18:1}$ |
| 6a | c(RGDfK) | GGGGG | - |
| 6b | c(RGDfK) | GGGGG | $C_{18:1}$ |

Further investigation of the NCL reaction showed how the conversion from starting free peptides into the dioleoyl peptide derivatives (dilipidated products) starts to become evident at 4h, with a complete conversion after overnight reaction (Figure 3). The single-tail lipopeptide intermediates (monolipidated products) were not quantifiable under ELSD since the "reloading" step happens rapidly after the formation of the amide bond ligated products.
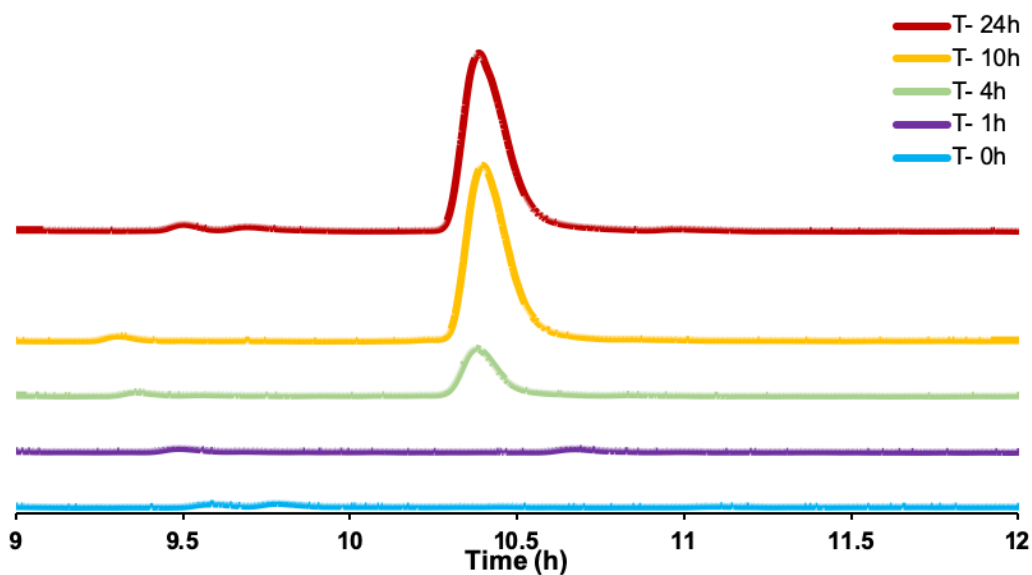
**Figure 3.** HPLC-ELSD traces monitoring the formation of dioleoyl-$C^5$GRGD (**5b**).

## 2.2. Characterization of Self-Assembling Lipopeptide Nanocarriers

As expected, neither the free peptides nor the oleoyl MESNA formed membranes in aqueous solution. However, the purified dioleoyl peptide products, when hydrated, readily formed micron-sized vesicles. Lipopeptide vesicular structures were identified by fluorescence microscopy using the membrane-staining dye Nile Red (Figure 4). Corroboration of the vesicular architecture was also achieved by transmission electron microscopy (TEM) (Figure 5).
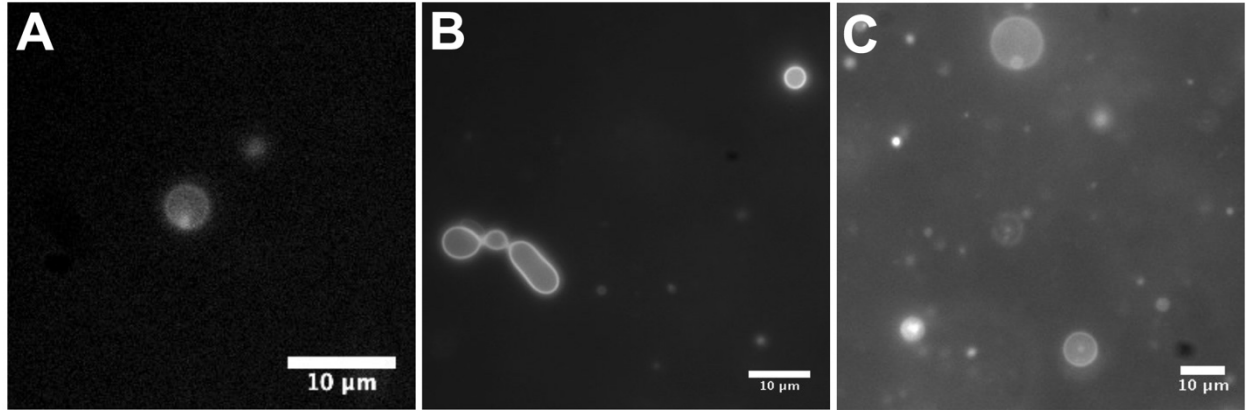
**Figure 4.** Fluorescence microscopy images of lipopeptide vesicles. A) dilipidated-CRGD (**1b**). B) dilipidated-C$^5$GRGD (**5b**). C) dilipidated-CGHK (**2b**) vesicles. All images were collected under similar instrumental conditions.
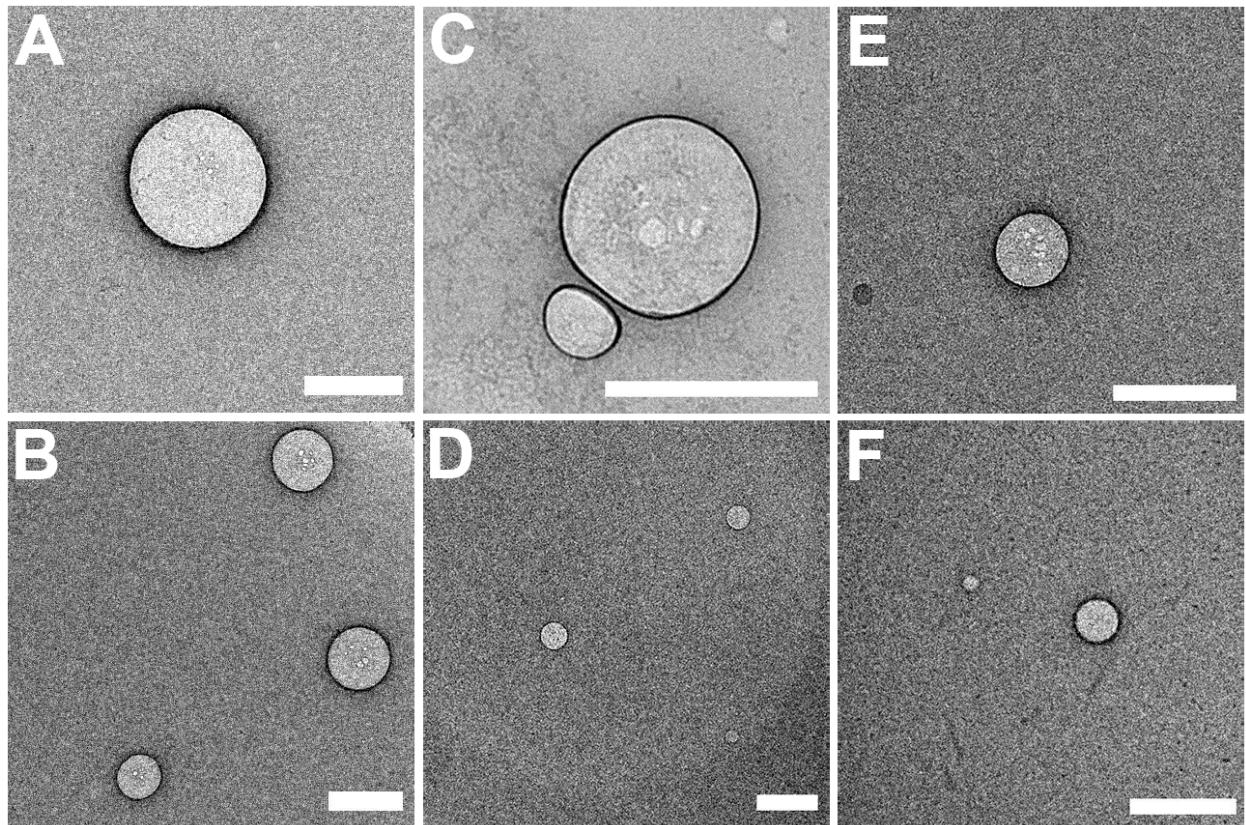


**Figure 5.** Transmission Electron Microscopy (TEM) images of lipopeptide vesicles. (A, B) dilipidated-C$^5$Gc(RGDfK)/CRGD (**6b/1b**) [ratio 1:2]. (C,D) dilipidated-C$^5$GRGD/CRGD (**5b/1b**) [ratio 1:2]. (E, F) dilipidated-CRGD (**1b**). Scale bars denote 500 nm.

## 2.3. Encapsulation of Biomolecules into Self-Assembling Lipopeptide Nanocarriers

The efficient encapsulation ability of the dioleoyl peptide vesicles was first determined by the inclusion of a neutral hydrophilic fluorophore, Texas-Red Dextran 10,000, in the hydration media, followed by vesicle characterization using fluorescence microscopy (Figure 6A). Proteins, such as sfGFP, were also encapsulated using a similar strategy (Figure 6B).

Once we demonstrated the high encapsulation efficiency of our lipopeptide vesicles, we next evaluated the compatibility to load therapeutic agents, such as DOX. DOX is one of the most commonly used therapeutics for the treatment of various cancers, including many types of carcinomas and soft tissue sarcomas.[13] This cell-permeable small molecule presents enhanced fluorescence upon binding to nucleic acid in cells. Further intercalation into DNA ultimately results in cell apoptosis. Lipopeptides were hydrated overnight at 37 ºC in PBS (pH 7.4) containing DOX [lipopeptide/drug (1:0.2)]. Vesicle formation was observed by fluorescence microscopy (Figure 6C). We next extruded the samples through a polycarbonate filter (100 nm) followed by the removal of un-encapsulated DOX using size-exclusion chromatography (Sephadex G-25). UV-Vis spectroscopy was employed to determine the final concentration of the encapsulated DOX.
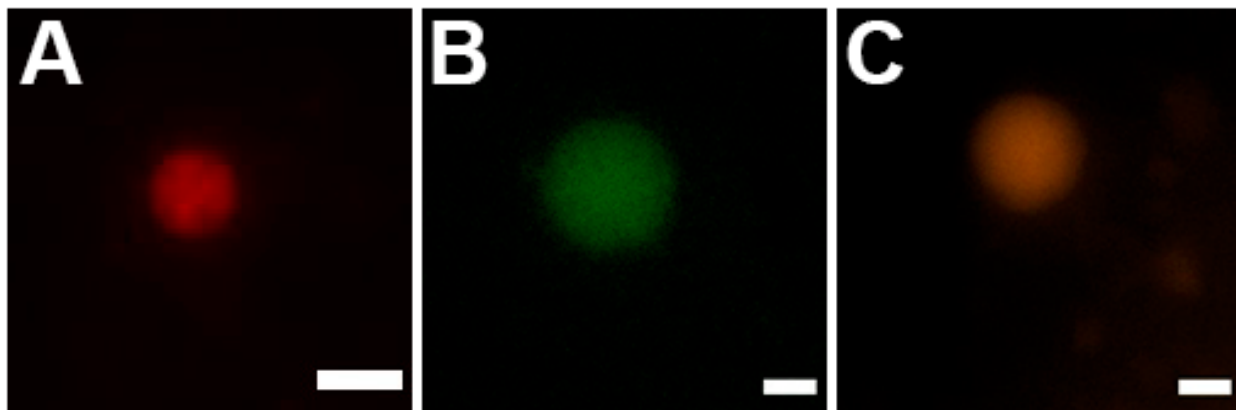
**Figure 6.** Fluorescence microscopy images showing the encapsulation of (A) Texas-Red Dextran into dioleoyl-C$^5$GRGD (**5b**) vesicles, (B) sfGFP and (C) DOX into dioleoyl-C$^5$GRGD/CRGD (**5b/1b**) vesicles. Scale bars denote 5 μm.

## 2.4. Cell Viability Studies

WST-1 cell viability assays were initially performed in order to assess the potential cytotoxicity of the lipopeptides. The viability assays showed that the lipopeptides show relatively low toxicity towards HeLa cells. $1 \times 10^4$ cells/well were seeded on a 96-well plate and incubated overnight prior to performing cell viability assay. The assay showed around 70% viable cells at high concentrations (250 μM) after 24 h of incubation.

## 2.5. Drug Delivery Mediated by Self-Assembling Lipopeptide Nanocarriers

We next evaluated the delivery ability of the self-assembled nanocarriers. As previously mentioned, our model system was based on cargo transport through integrin-mediated endocytosis. Initially, lipopeptides containing an RGD sequence were incubated with integrin-rich cell lines, such as HeLa ($\alpha_v\beta_3$ and $\alpha_v\beta_5$) and U87MG ($\alpha_v\beta_3$). The trimer sequence would allow specific

delivery of biomacromolecules (dextrans and/or drugs) to cancer cells overexpressing $\alpha_v\beta_3$ integrins. To demonstrate the main role of this motif in guiding the association of lipopeptide nanocarriers to $\alpha_v\beta_3$ integrin-rich tumor cells, U87MG cells were treated with dioleoyl-CRGD (**1b**) vesicles containing a fluorescent molecule, Texas-Red Dextran. Unfortunately, minimal significant delivery was observed by fluorescence microscopy. We next designed a new class of self-assembling lipopeptides, such as dioleoyl-C$^5$GRGD (**5b**) and dioleoyl-C$^5$Gc(RGDfK) (**6b**). Incorporation of flexible oligoglycine spacers would allow efficient spatial arrangement of the RGD sequences for enhanced cell adhesion. Additionally, cyclic peptide moieties have been reported to have a better anchorage on the cell integrin, due to their rigid conformation and structure.[20] Consequently, fluorescence microscopy experiments with **6b** and **1b** lipopeptide-based vesicles demonstrated better delivery of the encapsulated fluorescently-labeled dextran. To further improve the active transport of the cargo, the oligoglycine lipopeptides (**6b** and **5b**) were initially mixed with **1b** in a ratio of 1:2 or 1:5. Mixing both types of lipopeptides (with and without oligoglycine spacer) should facilitate an even better distribution of the RGD motifs, which could improve the specific recognition and adhesion to the $\alpha_v\beta_3$ integrin. Thus, enhanced cellular uptake was observed for lipopeptide mixtures compared to those composed of exclusively one peptide sequence (Figures 7 and 8).
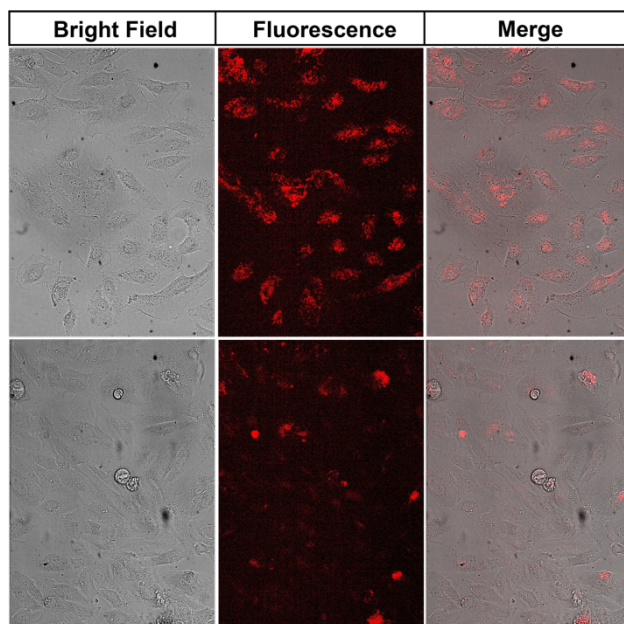
**Figure 7.** Confocal microscopy images showing HeLa cells treated with Texas-Red Dextran-encapsulated dioleoyl-C$^5$GRGD/CRGD (**5b/1b**) [ratio 1:2] nanocarriers at 37 $^o$C for 24 h. *Top*, in absence of any pre-treatment. *Bottom*, pre-treatment with free C$^5$GRGD (**5a**) peptide for 1 h. All images were collected under similar instrumental conditions.
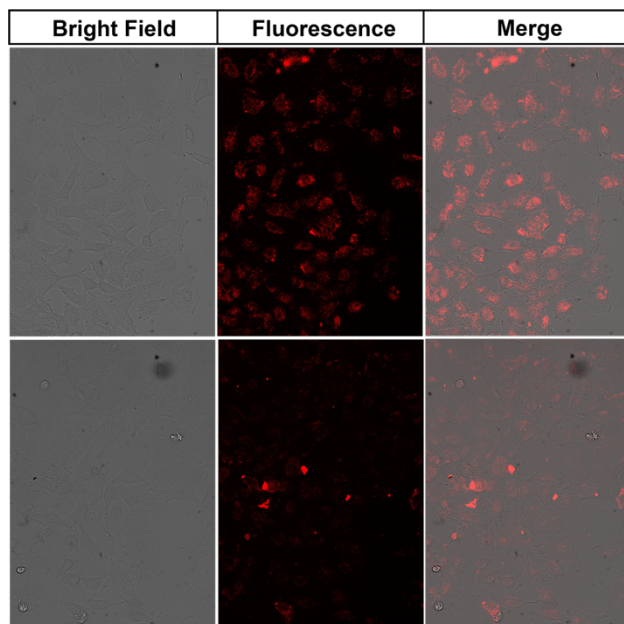


**Figure 8.** Confocal microscopy images showing HeLa cells treated with Texas-Red Dextran-encapsulated dioleoyl-C$^5$Gc(RGDfK)/CRGD (**6b/1b**) [ratio 1:2] nanocarriers at 37 °C for 24 h. *Top*, in absence of any pre-treatment. *Bottom*, pre-treatment with free C$^5$Gc(RGDfK) (**6a**) peptide for 1 h. All images were collected under similar instrumental conditions.

13

Verification that RGD sequence is the driving force of the specific recognition was obtained by conducting analogous experiments using lipopeptides containing CGHK and $C^5$GGHK sequences (**2b** and **4b**, respectively). The GHK sequence, unlike RGDs, lacks specific $\alpha_v\beta_3$-integrin binding affinity. Therefore, cargo delivery should be minimized as a consequence of the specificity absence. For instance, the selective uptake of the encapsulated endocytosis marker, Texas-Red Dextran 10,000, showed significantly less fluorescence signals for the mixture dioleoyl-$C^3$GGHK/dioleoyl-CGHK (**4b/2b**) [ratio 1:2] (Figure 9).
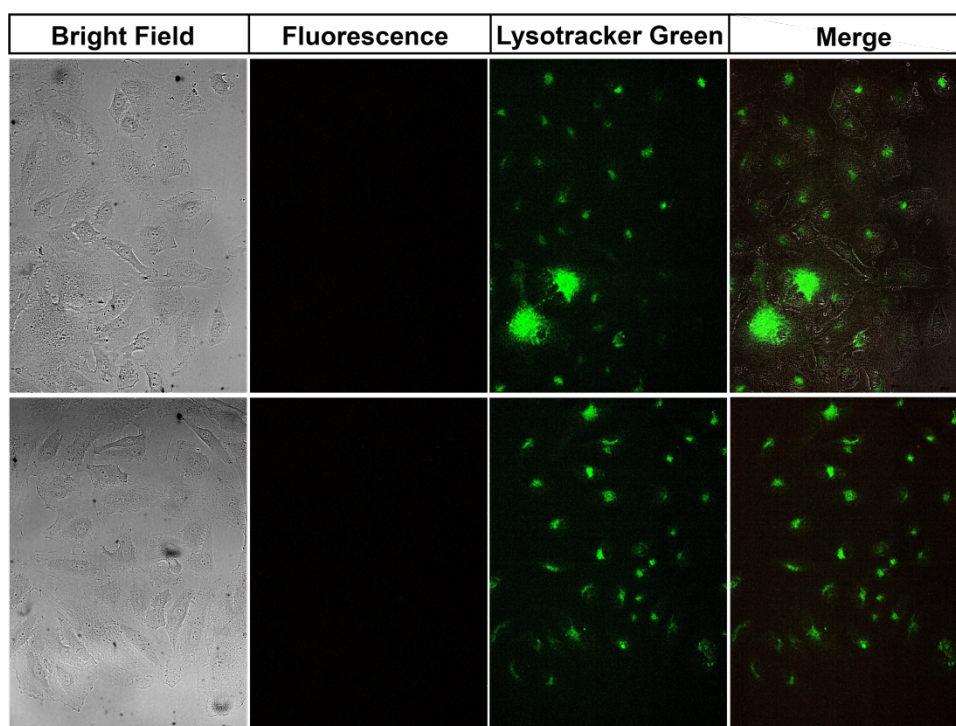


**Figure 9.** Confocal microscopy images showing HeLa cells treated with Texas-Red Dextran-encapsulated dioleoyl-$C^3$GGHK/CGHK (**4b/2b**) [ratio 1:2] nanocarriers at 37 °C for 24 h. *Top*, in absence of any pre-treatment. *Bottom*, pre-treatment with free $C^3$GGHK (**4a**) peptide for 1 h. All images were collected under similar instrumental conditions.

The cyclic and linear RGD-based peptides containing oligoglycine spacers were selected as targeting ligands to be conjugated onto the lipid tails. In particular, the lipopeptide mixtures of dioleoyl-$C^5$Gc(RGDfK)/CRGD (**6b/1b**) [ratio 1:5] and/or dioleoyl-$C^5$GRGD/CRGD (**5b/1b**)

[ratio 1:5] were designed to improve the desired specific delivery of DOX to U87MG cancer cells overexpressing $\alpha_v\beta_3$ integrins. Confocal laser scanning microscopy (CLSM) was employed to evaluate cellular uptake behavior of the nanocarriers against the $\alpha_v\beta_3$ receptor-positive U87MG cells. Figure 10 and 11 (*top*) shows images of U87MG cells incubated with DOX-encapsulated targeted lipopeptide (**5b/1b** and **6b/1b**, respectively) [ratio 1:5] vesicles. DOX concentration used for this study was 5 µM. For comparison, cells were pre-incubated with free RGD peptides (**5b** and **6b**) for 1 h prior to the treatment of the vesicles with DOX. Cells pre-blocked with free RGD peptides only displayed faint fluorescent signals under the same instrumental conditions (Figure 10 and 11, *bottom*). Based on the fluorescence intensity, the efficiency of cellular uptake decreased in the order of free DOX, DOX-loaded lipopeptide vesicles, and integrin blocked cells. Enhanced cellular uptake exhibited by the RGD functionalized lipopeptide vesicles describe receptor-mediated endocytosis pathway. It is evident that treatment of cells with the lipopeptide nanocarriers results in a significantly decreased level of cell viability when compared to the free peptide treated, integrin blocked cells. Most of the red fluorescence was observed within $\alpha_v\beta_3$ integrin-rich U87MG cells, with very little on the cells' periphery, indicative of successful internalization of the DOX-encapsulated lipopeptide vesicles. The morphology of the cells treated with lipopeptide carriers and free peptides appear to be similar at 48 h with 5 µM DOX concentrations. A significant portion of cells became rounded and non-adherent, indicating cell apoptosis. On the contrary, rounded and detached cells were not visualized in cells treated with lipopeptide vesicles encapsulating Texas-Red Dextran 10,000. This further suggests that the anticancer activity of the lipopeptide nanovesicular structure containing DOX is related to the encapsulated drug, corroborating WST-1 assay results of plain lipopeptides.
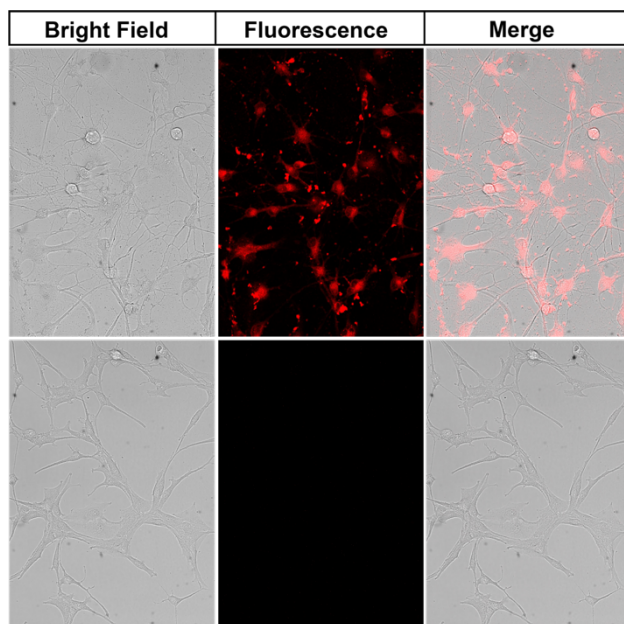
**Figure 10.** Confocal microscopy images showing U87MG cells treated with DOX-encapsulated dioleoyl-C$^5$GRGD/CRGD (**5b**/**1b**) [ratio 1:5] nanocarriers at 37 °C for 24 h. *Top*, in absence of any pre-treatment. *Bottom*, pre-treatment with free C$^5$GRGD (**5a**) peptide for 1 h. All DOX final concentrations are 5 µM. All images were collected under similar instrumental conditions.
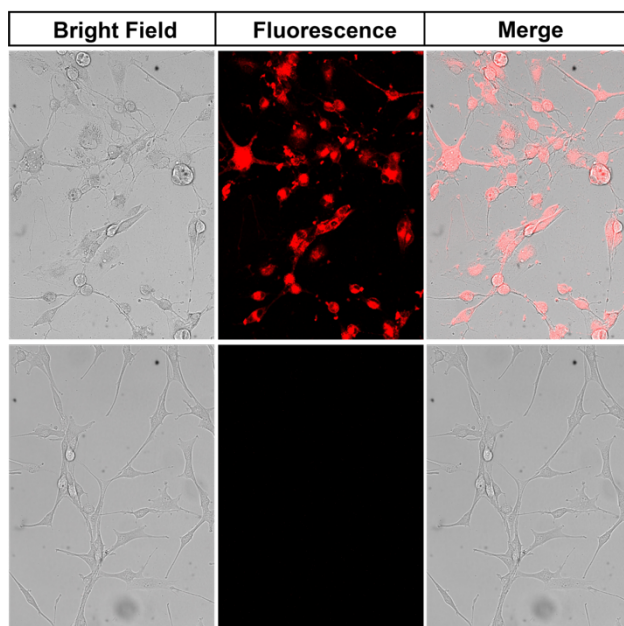


**Figure 11.** Confocal microscopy images showing U87MG cells treated with DOX-encapsulated dioleoyl-C$^5$Gc(RGDfK)/CRGD (**6b**/**1b**) [ratio 1:5] nanocarriers at 37 °C for 24 h. *Top*, in absence of any pre-treatment. *Bottom*, pre-treatment with free C$^5$Gc(RGDfK) (**6a**) peptide for 1 h. All DOX final concentrations are 5 µM. All images were collected under similar conditions.

## 3. CONCLUSIONS

In summary, we have designed, synthesized and characterized a novel class of self-assembling lipopeptides using native chemical ligation (NCL) between various N-terminal cysteine-containing peptides and oleoyl MESNA thioester. Remarkably, this catalyst-free methodology allowed for the construction of functional lipopeptides conjugated to integrin-binding motifs, which are capable of spontaneously self-assembly into vesicles. The resulting lipopeptide nanocarriers enhance cellular uptake via receptor-mediated endocytosis pathway. We foresee future applications of our straightforward methodology for the construction of biocompatible, robust and nontoxic vehicles. These model systems can be used not only as targeted drug delivery platforms but also as advanced synthetic cells.

# 4. EXPERIMENTAL SECTION

## 4.1. Materials

9-fluorenylmethoxycarbonyl (Fmoc) protected amino acids, 4-methylpiperidine, thioanisole, ethanedithiol (EDT) tetrakis(triphenylphosphine) palladium, phenylsilane, trifluoroacetic acid (TFA), *N,N*-ethyldiisopropylamine, acetonitrile (ACN), *N,N*-dimethylformamide (DMF), dichloromethane (DCM), phenol, methanol (MeOH) and ethanol (EtOH) were purchased from Sigma Aldrich (USA). 2-chlorotrityl chloride (CTC) resin, 2,2,4,6,7-tetramethyluronium hexafluorophosphate (HBTU), 1-[bis(dimethylamino)methylene]-1H-1,2,3-triazolo[4,5-b]pyridinium 3-oxide hexafluorophosphate (HATU) and 1-hydroxybenzotriazole hydrate (HOBt) were purchased from Chem Impex (USA. All the commercially available chemical regents were used without further purification.

Reagent K (cleavage cocktail) contains 82.5% (v/v) TFA, 5% (v/v) $H_2O$, 5% (v/v) phenol, 5% (v/v) thioanisole, and 2.5% (v/v) ethanedithiol.

## 4.2. Instrumentation

Analytical reverse phase high-performance liquid chromatography (RP-HPLC) was carried out on an Agilent 1100 series system with an Eclipse Plus C8 analytical column. The eluent has a gradient from *Phase A* ($H_2O$ with 0.1%TFA) to *Phase B* (MeOH with 0.1% TFA). Semi-preparative RP-HPLC purification was carried out on Zorbax SB-C18 semi-preparative column with *Phase A* ($H_2O$ with 0.1% TFA) and *Phase B* (MeOH or ACN with 0.1% TFA). High-

resolution mass spectra (HR-MS) were obtained at the Molecular Mass Spectrometry Facility (MMSF) of the University of California, San Diego. A NanoDrop 2000C spectrophotometer was used for UV-vis measurements. Micrographs were observed in an inverted optical microscope (Axiovert 200, Zeiss, Germany) or a laser confocal scanning microscope (Olympus, FV1000, Japan).

## 4.3. Lipopeptide Synthesis

### 4.3.1. Synthesis of linear peptides

I.      Attachment of first Fmoc-amino acid to 2-chlorotrityl-chloride resin

CTC resin was treated with a solution of the first Fmoc-amino acid (1.5 equiv) in anhydrous DCM containing DIPEA (5 equiv) at room temperature for 2 h. Afterward, the resin was subsequently washed with DMF (3 × 5 mL), DCM (3 × 5 mL), and DCM/DIEA/MeOH (17:2:1; 3 × 5 mL). After capping free sites with MeOH, the resin was dried under vacuum overnight to obtain Fmoc-amino acid bound on the resin.

II.     Fmoc deprotection

A solution of 20% piperidine in DMF (2 mL) was added to Fmoc protected amino acid on resin, and the reaction mixture was shaken for 30 min. The resin was then washed with DMF (3 × 5 mL).

III.    Coupling of amino acids

Fmoc-protected amino acids (4 equiv) were sequentially coupled to the resin to obtain the desired peptides. Amino acids were first dissolved in DMF, then HBTU (4 equiv), HOBt (4 equiv) and DIPEA (8 equiv) were added. The mixture was added to the resin and the resulting suspension was shaken at room temperature for 1 h. Afterward, the resin was washed with DMF (3 × 5 mL). Cycles of amino acid couplings and washing were repeated until the synthesis of the final peptidyl resins. Evaluation of the sequences was performed by cleaving 2 mg of the resin with a solution of HFIP/DCM (1:4; 500 µL) and monitoring the free protected peptides by RP-HPLC/MS (Eclipse Plus C8 analytical column, 5-30% ACN in $H_2O$ with 0.1% TFA, 0-5 min; 30-95% ACN in $H_2O$ with 0.1% TFA, 5-20min).

IV.     Deprotection and cleavage of the resin with cocktail reagent K

After Fmoc removal of the final amino acid (Cys), the peptide-grafted resin was washed with DMF (3x), DCM (3x), and MeOH (3x) and dried under vacuum. The protecting groups of the peptides were removed by adding the cocktail solution reagent K: TFA/phenol/thioanisole/$H_2O$/EDT (82.5:5.0:5.0:2.5) and followed by stirring for 3 h. The reaction solution was then filtered, and the filtrates were collected in Eppendorf tubes. The resulting solutions were treated with cold diethyl ether and then centrifuged (3 cycles) to yield the final deprotected peptide. Peptides were further purified by semi-preparative RP-HPLC (Zorbax SB-C18 semi-preparative column, 5-30% ACN in $H_2O$ with 0.1% TFA, 0-5 min; 30-95% ACN in $H_2O$ with 0.1% TFA, 5-30min) to yield white powders.

Note: The cyclic peptide $C^5Gc(RGDfK)$ [6a] was prepared following a similar SPPS protocol. Cyclization step was carried out in solution phase after cleaving the peptidyl resin.

### *4.3.2. Lipidation of Peptides*

The purified peptide (1 equiv) and MESNA thiolate (2 equiv) **7** [previously prepared following literature procedures][18] were dissolved in a solution of 100 mM Tris.HCl pH 8.0 buffer containing 10 mM of TCEP.HCl. The mixture was stirred overnight. At various time points, aliquots of the sample were diluted to 100 µL with MeOH to analyze product formation by HPLC/ELSD/MS using an Eclipse Plus C8 analytical column at a flow rate of 1.0 mL/min. The reaction mixture was filtered using a 0.2 um syringe-driven filter. The crude solution was then purified by semi-preparative RP-HPLC (Zorbax SB-C18 semi-preparative column, 50-95% MeOH in $H_2O$ with 0.1% TFA, 0-15 min). The desired lipopeptides were obtained as colorless films.

### 4.4. Encapsulation Experiments

I.     Hydration of Lipid Film

An aliquot of 100 µL of a 2.5 mM solution of dioleoyl-peptide in MeOH was added to a 0.5 mL vial, placed under Ar, and dried to prepare a lipopeptide film. Then, 100 µL of PBS 1x containing the desired fluorescent biomolecule (Texas Red dextran, DOX or GFP) were added, and the solution was tumbled for 12 h.

II.     Sonication and Dialysis

The hydrated lipid film was sonicated for 1 h at room temperature. The resulting mixture was then dialyzed to remove excess non-encapsulated fluorescent biomolecule by loading the

solution on a floating 25 mm diameter, Type-VS Millipore membrane (MF type, VS filter, mean pore size = 0.025 μm, Millipore, Inc.). Biomolecule-encapsulated vesicles were examined by fluorescence microscopy.

## 4.5. Cell culture

HeLa and U87MG cells obtained from ATCC were cultured in DMEM supplemented with penicillin (50 units/mL), streptomycin (50 μg/mL) and 10% FBS at 37 ºC and 5% $CO_2$.

## 4.6. Microscopy

I.      Optical and Confocal Microscopy

Lipopeptide vesicle imaging was performed on an Olympus BX51 optical microscope and an Axio Observer Z1 inverted microscope (Carl Zeiss Microscopy Gmb, Germany) with Yokogawa CSU-X1 spinning-disk confocal unit.

II.      Transmission Electron Microscopy (TEM)

Micrographs were recorded on an FEI Tecnai Sphera microscope operating at 200 kV and equipped with a LaB6 electron gun using the standard cryotransfer holders developed by Gatan. Copper grids (Formvar/carbon-coated, 400 mesh copper) were glow discharged at 20 mA for 1.5 min. After this, 4.0 μL of a solution of the lipopeptide in $H_2O$ was added to the grid surface and allowed to sit for ∼10 s. It was washed with 10 drops of $H_2O$ and subsequently stained with three drops of 1% uranyl acetate. The staining was carried out for ∼10 s before blotting with filter paper.

Following this, samples were imaged by transmission electron microscopy (TEM) and processed using Image J.

## 4.7. Live-Cell Imaging

HeLa and U87MG cells were plated (30,000 cells/well and 20,000 cell/well, respectively) in an 8-well Lab-Tek chamber slide (ThermoFisher) and allowed to adhere overnight at 37 ºC and 5% $CO_2$. Cells were then treated with biomolecule (Texas Red-Dextran 3,000 or DOX)-encapsulated lipopeptides. These nanocarriers were previously diluted with OptiMEM media to achieve the desired biomolecule concentrations.

Cells were imaged on the Carl Zeiss Axio Observer Z1 inverted microscope with Yokogawa CSU-X1 spinning-disk confocal unit using 20x, 0.8 NA objective to an ORCA-Flash 4.0 V2 Digital CMOS camera (Hamamatsu, Japan). An incubation chamber with temperature and $CO_2$ control (World Precision Instruments) was used for live-cell imaging. In particular, 37 ºC and 5% $CO_2$ in the incubator chamber (Labtek) were chosen as imaging conditions. Images were acquired using Zen Blue software (Carl Zeiss) and processed using Image J.

This thesis in full is currently being prepared for submission for publication of the material. Cho, Christy J.; Brea, Roberto J.; Devaraj, Neal K. "Self-Assembling Lipopeptide Nanocarriers for Targeted Cellular Uptake". Ms. Cho was the principal researcher/author on this paper.

## 5. REFERENCES

[1]     Mirza, A. Z. & Siddiqui, F. A. Nanomedicine and drug delivery: a mini review. *Int. Nano Lett.* **4**, (2014).

[2]     Sinha, R., Kim, G. J., Nie, S. & Shin, D. M. Nanotechnology in cancer therapeutics: Bioconjugated nanoparticles for drug delivery. *Mol. Cancer Ther.* **5**, 1909-1917 (2006).

[3]     Tran, S., DeGiovanni, P.-J., Piel, B. & Rai, P. Cancer nanomedicine: a review of recent success in drug delivery. *Clin. Transl. Med.* **6**, (2017).

[4]     Wicki, A., Witzigmann, D., Balasubramanian, V. & Huwyler, J. Nanomedicine in cancer therapy: challenges, opportunities, and clinical applications. *J. Control. Release* **200**, 138-157 (2015).

[5]     Gelperina, S., Kisich, K., Iseman, M. D. & Heifets, L. The potential advantages of nanoparticle drug delivery systems in chemotherapy of tuberculosis. *Am. J. Respir. Crit. Care Med.* **172**, 1487-1490 (2005).

[6]     Yang, X., Li, Z., Li, M., Ren, J. & Qu, X. Fluorescent protein capped mesoporous nanoparticles for intracellular drug delivery and imaging. *Chem. - A Eur. J.* **19**, 15378-15383 (2013).

[7]     Stroh, M., Zimmer, J. P., Duda, D. G., Levchenko, T. S., Cohen, K. S., Brown, E. B., Scadden, D. T., Torchilin, V. P., Bawendi, M. G., Fukumura, D. & Jain, R. K. Quantum dots spectrally distinguish multiple species within the tumor milieu in vivo. *Nat. Med.* **11**, 678-682 (2005).

[8]     Trivedi, R. & Kompella, U. B. Nanomicellar formulations for sustained drug delivery. *Nanomedicine* **5**, 485-505 (2011).

[9]     Pattni, B. S., Chupin, V. V. & Torchilin, V. P. New developments in liposomal drug delivery. *Chem. Rev.* **115**, 10938-10966 (2015).

[10]    Cho, K., Wang, X., Nie, S., Chen, Z. & Shin, D. M. Therapeutic nanoparticles for drug delivery in cancer. *Clin. Cancer Res.* **14**, 1310-1316 (2008).

[11]    Dunehoo, A. L., Anderson, M., Majumdar, S., Kobayashi, N., Berkland, C. & Siahaan, T. J. Cell adhesion molecules for targeted drug delivery. *J. Pharm. Sci.* **95**, 1856-1872 (2006).

[12]    Zhang, L., Zhu, S., Qian, L., Pei, Y., Qiu, Y. & Jiang, Y. RGD-modified PEG-PAMAM-DOX conjugates: In vitro and in vivo studies for glioma. *Eur. J. Pharm. Biopharm.* **79**, 232-240 (2011).

[13] Wang, Y., Cao, X., Guo, R., Shen, M., Zhang, M., Zhu, M. & Shi, X. Targeted delivery of doxorubicin into cancer cells using a folic acid-dendrimer conjugate. *Polym. Chem.* **2**, 1754-1760 (2011).

[14] Choi, S. K. Thomas, T., Li, M. H., Kotlyar, A., Desai, A. & Baker, J. R. Jr. Light-controlled release of caged doxorubicin from folate receptor-targeting PAMAM dendrimer nanoconjugate. *Chem. Commun.* **46**, 2632-2634 (2010).

[15] Nasongkla, N. Shuai, X., Ai, H., Weinberg, B. D., Pink, J., Boothman, D. A. & Gao, J. cRGD-functionalized polymer micelles for targeted doxorubicin delivery. *Angew. Chem. Int. Ed.* **43**, 6323-6327 (2004).

[16] Dawson, P. E., Muir, T. W., Clark-Lewis, I. & Kent, S. B. Synthesis of proteins by native chemical ligation. *Science* **266**, 776-779 (1994).

[17] Vázquez, O. & Seitz, O. Templated native chemical ligation: peptide chemistry beyond protein synthesis. *J. Pept. Sci.* **20**, 78-86 (2014).

[18] Brea, R. J., Cole, C. M. & Devaraj, N. K. In situ vesicle formation by native chemical ligation. *Angew. Chem. Int. Ed.* **53**, 14102-14105 (2014).

[19] Palomo, J. M. Solid-phase peptide synthesis: an overview focused on the preparation of biologically relevant peptides. *RSC Adv.* **4**, 32658-32672 (2014).

[20] Lai, Y., Xie, C., Zhang, Z., Lu, W. & Ding, J. Design and synthesis of a potent peptide containing both specific and non-specific cell-adhesion motifs. *Biomaterials* **31**, 4809-4817 (2010).